Published online 23 January 2020 *Nucleic Acids Research, 2020, Vol. 48, No. 5* ***2473–2485***
doi: 10.1093/nar/gkz1242

Cockayne syndrome group A and B proteins function in rRNA transcription through nucleolin regulation

Mustafa N. Okur[1], Jong-Hyuk Lee[1], Wasif Osmani[1], Risako Kimura[1], Tyler G. Demarest[1], Deborah L. Croteau[1] and Vilhelm A. Bohr[1,2,*]

[1]Laboratory of Molecular Gerontology, National Institute on Aging, National Institutes of Health, Baltimore, MD 21224, USA and [2]Danish Center for Healthy Aging, University of Copenhagen, Blegdamsvej 3B, 2200 Copenhagen N, Denmark

Received November 21, 2018; Revised December 30, 2019; Editorial Decision December 31, 2019; Accepted December 31, 2019

ABSTRACT

Cockayne Syndrome (CS) is a rare neurodegenerative disease characterized by short stature, accelerated aging and short lifespan. Mutations in two human genes, *ERCC8/CSA* and *ERCC6/CSB*, are causative for CS and their protein products, CSA and CSB, while structurally unrelated, play roles in DNA repair and other aspects of DNA metabolism in human cells. Many clinical and molecular features of CS remain poorly understood, and it was observed that CSA and CSB regulate transcription of ribosomal DNA (rDNA) genes and ribosome biogenesis. Here, we investigate the dysregulation of rRNA synthesis in CS. We report that Nucleolin (Ncl), a nucleolar protein that regulates rRNA synthesis and ribosome biogenesis, interacts with CSA and CSB. In addition, CSA induces ubiquitination of Ncl, enhances binding of CSB to Ncl, and CSA and CSB both stimulate the binding of Ncl to rDNA and subsequent rRNA synthesis. CSB and CSA also increase RNA Polymerase I loading to the coding region of the rDNA and this is Ncl dependent. These findings suggest that CSA and CSB are positive regulators of rRNA synthesis via Ncl regulation. Most CS patients carry mutations in CSA and CSB and present with similar clinical features, thus our findings provide novel insights into disease mechanism.

INTRODUCTION

Cockayne Syndrome (CS) is a rare, autosomal recessive neurodegenerative disorder characterized by short stature, cachexia, photosensitivity, progressive hearing and vision loss, premature aging and short life span (1). Mutations linked to CS are predominantly in the genes *ERCC8/CSA* and *ERCC6/CSB*, although mutations in *XPB, XPD* and *XPG* can cause CS-like features. CSA, CSB, XPB, XPD and XPG participate in transcription-coupled nucleotide excision repair (TC-NER) (2–5). CSA contains multiple WD40 motifs and is a component of an E3 ubiquitin ligase complex that also includes Cul4A, DDB1 and RBX1. CSB is a member of the SWI2/SNF2 family of DNA-dependent ATPases and contains a highly conserved C-terminal ubiquitin-binding domain (UBD) that plays roles in promoting cell survival and recovery of transcription after DNA damage and oxidative stress (6–8). CSB is a nuclear protein that localizes predominantly to the nucleolus. CSA is primarily localized to the nucleoplasm, with limited abundance in the nucleolus. However, a recent study reported that CSA relocates to and becomes highly enriched in the nucleolus in cells treated with a proteasome inhibitor (9). This suggests that CSA may be targeted for degradation in the nucleolus.

The nucleolus is the sub-compartment of the nucleus in which rDNA is transcribed, pre-rRNA is processed, and ribosome assembly begins (10,11). The nucleolus itself has three sub-compartments: the fibrillar center (FC), the dense fibrillar center (DFC) and the granular center (GC). rDNA is transcribed at the interface between the FC and DFC, and pre-rRNA processing and ribosome subunit assembly largely occur in the DFC (12). Due to its role in ribosome biogenesis, the nucleolus indirectly regulates cell proliferation and the cellular stress response (13). Dysregulation of nucleolar functions is associated with human diseases characterized by growth defects, neurodegeneration and premature aging (14,15).

Recent studies suggest that CSA and CSB regulate early steps of rDNA transcription, the rate-limiting step of ribosome biogenesis (16,17). CS proteins interact with RNA polymerase I (Pol I) and are required for efficient synthesis of pre-rRNA (47S in mammals), which is processed to mature 5.8S, 18S and 28S rRNA (9,18,19). Here, we provide evidence that mutations in the CSB UBD inhibit the synthesis of pre-rRNA and we demonstrate that the CSB UBD is required for the specific interaction of CSB with Nucleolin (Ncl). Ncl is an abundant nucleolar protein localized to the

*To whom correspondence should be addressed. Tel: +1 410 558 8162; Email: vbohr@nih.gov

DFC and GC (20). We also demonstrate that CSA binds to and promotes the ubiquitination of Ncl, enhances the interaction between Ncl and CSB and that CSA and CSB promote binding of Ncl to rDNA to regulate rDNA transcription. Moreover, we show that the increase in relative Pol I binding to the 3′-end of rDNA coding repeat (H13) by CSB or CSA expression is Ncl-dependent. Although CSA and CSB have defined roles in TC-NER, the complex clinical features of CS suggest that a DNA repair deficiency may not be the only explanation for CS pathology. Since CSA and CSB patient clinical features are similar, insight into where the functions of these two proteins converge should provide particularly important insight into CS disease mechanisms.

MATERIALS AND METHODS

Cell culture and cell line construction

Cells were cultured in Dulbecco's modified Eagle medium (DMEM) containing 10% fetal bovine serum (FBS) and 1% penicillin/streptomycin in a humidified chamber under 5% CO_2 at 37°C. CS1AN cells, SV40-transformed CS patient cells carry mutations in CSB, were stably transfected with GFP vector control, GFP-CSB^{WT} or GFP-CSB$^{UBDmut.}$ ($L_{1427}L_{1428}\rightarrow G_{1427}G_{1428}$) using JetPrime reagent (Polyplus-transfection, Illkirch, France) according to the manufacturer's recommendations. Transfected cells were grown under selection for resistance to 800 μg/ml geneticin (Teknova) for 2 weeks, and then transferred to and maintained in media containing 400 μg/ml geneticin. The expression levels of CSB^{WT} and CSB$^{UBDmut.}$ were similar to endogenous CSB expression levels in CS3BE patient-derived fibroblasts (Supplementary Figure S1). Plasmids expressing GFP-CSB^{WT}, GFP-CSB$^{UBDmut.}$ and SV40-transformed CSA-deficient CS3BE cells stably expressing vector control or pcDNA-CSA^{WT} were the generous gifts of Dr David M. Wilson, III (8).

siRNA knockdown

siRNA was diluted with DMEM to a final concentration of 20 nM, mixed with INTERFERin (Polyplus transfection), incubated for 15 min at room temperature and transfected into target cells according to the manufacturer's instructions. Cells were lysed 3 days after transfection. siRNAs sequences were as follows: siERCC6 (5′-CCACUACAAU AGCUUCAAGACAGCC-3′), siERCC8 (5′-GGAGAA CAGAUAACUAUGCUUAAGG -3′), siNcl #1 (5′-AGAC UAUAGAGGUGGAAAGAAUAGC -3′), and siNcl #2 (5′-CCGUGUUGGUUUUGACUGGAUAUTC-3′).

Immunostaining

Cells were cultured in 4-well glass-bottom chamber slides (ThermoFisher, 154526PK Nunc™ Lab-Tek™ II Chamber Slide™), fixed with 4% paraformaldehyde in PBS at room temperature for 15 min, and permeabilized in PBS containing 0.3% Triton X-100 for 10 min on ice. Slides were incubated in 3% bovine serum albumin in PBS at RT for 1 h and then incubated with primary antibody (e.g. anti-nucleolin antibody; Santa Cruz, #sc-8031) diluted in PBS overnight at 4°C. Cells were washed with PBS and incubated with secondary antibody (ThermoFisher, Alexa Fluor® 594) at room temperature for 1 h, washed three times in PBS 0.05% Tween20 and mounted for imaging using ProLong™ Diamond Antifade Mountant with DAPI (ThermoFisher, #P36962). Cells were visualized by fluorescence microscopy (Zeis Observer Z.1, X-cite).

Immunoprecipitation, immunoblotting, deubiquitination, and mass spectrometry

Cells were lysed in IP lysis buffer (20 mM Tris-HCl, pH 7.4, 150 mM NaCl, 0.2% NP-40, 0.3% Triton-X-100, 1.5 mM $MgCl_2$) supplemented with Benzonase® Nuclease (Millipore, #70664-3) and 5 mM N-ethylmaleimide (Sigma, #E38760) unless indicated otherwise. GFP-Trap® A (Chromotek) was used to immunoprecipitate GFP fusion proteins. Antibodies used to immunoprecipitate endogenous antigens were as follows: CSB (H-300) (Santa Cruz, #sc-25370), CSA (Abcam, #ab137033) and Ncl (Millipore, #05-565). Protein ubiquitination was quantified as previously described (21,22). Antibodies were used according to the manufacturer's instructions to detect the following antigens: UB (Santa Cruz, #sc-8017), CSB (Santa Cruz, #sc-25370), Ncl (Santa Cruz, #sc-8031), CSA (Abcam, #ab137033), GAPDH (Abclonal, #AC027), DDB1 (Abcam, #ab109027).

Following immunoprecipitation, GFP-Trap® A beads were treated with 1.0 μM USP2 deubiquitinating enzyme (R&D systems; Recombinant Human USP2 Catalytic Domain; #E504) for 1 h at 37°C in 30 μl of USP2 buffer (50 mM HEPES pH 7.5, 100 mM $NaCl_2$, 2 mM DTT, 1 mM $MnCl_2$ and 0.01% (w/v) Brij-35). For mass spectrometry, cell extracts containing GFP-CSB^{WT} and GFP-CSB$^{UBDmut.}$ were analyzed by SDS-PAGE, stained with SilverQuest™ (ThermoFisher, #LC6070) and a total of five bands of interest were excised from gel (arrows in Figure 1F). Samples were submitted to Harvard Taplin Mass Spectrometry Facility for analysis by mass spectrometry. Unique peptide results from each gel slice are listed in Supplementary Table S1.

Cell growth

Growth characteristics of CS1AN cells expressing GFP, GFP-CSB^{WT}, and GFP-CSB$^{UBDmut.}$ were determined by using a Celligo® imaging automated cytometer. Briefly, 2000 cells/well were seeded in 96-well plates and incubated overnight. Cells were counted the next day by using cytometer and then growth characteristics of the cells were monitored and tracked every 24 h for the next 3 days via whole-well imaging and label-free bright field cell counting. The growth curve was generated by normalizing the initial cell counts on Day 1.

Quantitative real-time PCR (qPCR)

Total RNA was extracted from cells using TRIzol® (Invitrogen). One microgram of total RNA was reverse-transcribed using the iScript™ cDNA Synthesis Kit (Bio-Rad). qPCR was performed using the DyNAmo HS SYBR Green qPCR Kit (F-410L, ThermoFisher scientific) with

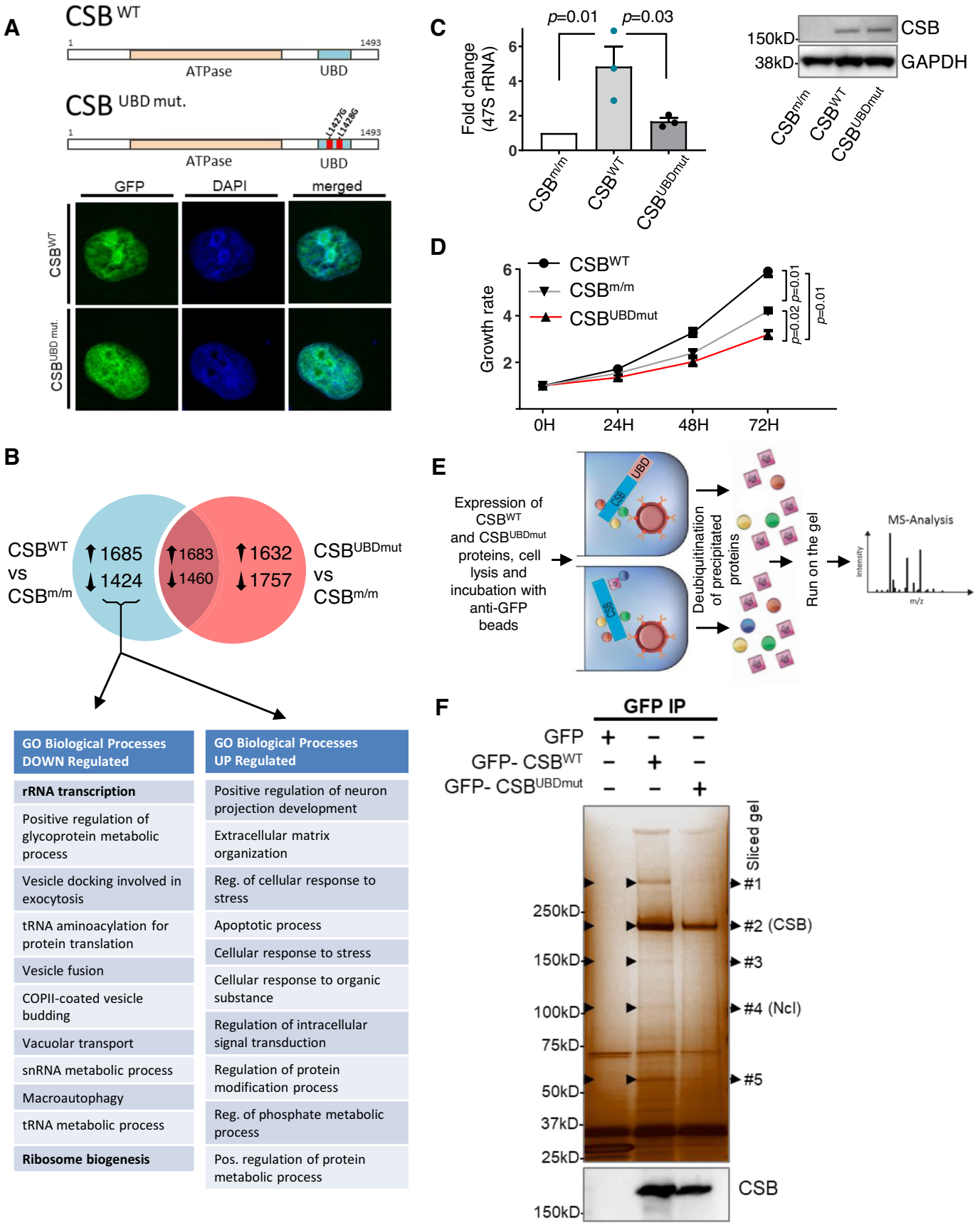

GO Biological Processes DOWN Regulated	GO Biological Processes UP Regulated
rRNA transcription	Positive regulation of neuron projection development
Positive regulation of glycoprotein metabolic process	Extracellular matrix organization
Vesicle docking involved in exocytosis	Reg. of cellular response to stress
tRNA aminoacylation for protein translation	Apoptotic process
Vesicle fusion	Cellular response to stress
COPII-coated vesicle budding	Cellular response to organic substance
Vacuolar transport	Regulation of intracellular signal transduction
snRNA metabolic process	Regulation of protein modification process
Macroautophagy	Reg. of phosphate metabolic process
tRNA metabolic process	Pos. regulation of protein metabolic process
Ribosome biogenesis	

Figure 1. UBD of CSB is required for nucleolar functions of CSB. (**A**) Schematic of the domain structure and localization of CSB^{WT} and $CSB^{UBDmut.}$ that possesses single-site mutations of $L_{1427}L_{1428} \rightarrow G_{1427}G_{1428}$. Representative images for GFP-tagged CSB^{WT} and GFP-tagged $CSB^{UBDmut.}$ that are stably

the CFX Connect Real-time PCR Detection System (Bio-Rad). Experimental values were normalized to values for GAPDH. Primer sequences used are listed in Supplementary Table S2. Quantifications were reported as an average ± standard error of the mean.

Chromatin immunoprecipitation (ChIP)

ChIP was performed as described (23), with slight modifications. Briefly, CS1AN cells were incubated in 1% formaldehyde PBS for 10 min at room temperature. The solution was brought to a final concentration of 0.125 M glycine, and cells were harvested by centrifugation, washed three times in cold PBS, then incubated in buffer A (5 mM PIPES (pH 8.0), 85 mM KCl, 0.5% NP-40, protease inhibitor cocktail (GenDEPOT, Katy, TX, U.S.A.)). Cell extracts were centrifuged, and pelleted material was resuspended in buffer B (100 mM Tris-Cl (pH 8.1), 1% sodium dodecyl sulfate (SDS), 10 mM EDTA, protease inhibitor cocktail). Chromatin was sheared using an S-450 sonicator (Branson, Danbury, CT, U.S.A.). An aliquot containing 500 μg DNA was diluted 10-fold in IP buffer (0.01% SDS, 1.1% Triton X-100, 1.2 mM EDTA, 16.7 mM Tris-Cl (pH 8.1), 167 mM NaCl and protease inhibitor cocktail) and incubated with primary antibody Nucleolin (Novus, #NB600-241) or RPA116 (Kindly provided by Dr. Holger Bernhard Bierhoff and Dr. Ingrid Grummt (24)) overnight at 4°C. Samples were incubated 2–4 h at 4°C with protein A - or protein G-linked agarose beads. Beads were washed sequentially with TSE150 (0.1% SDS, 1% Triton X-100, 2 mM EDTA, 20 mM Tris-Cl (pH 8.1), 150 mM NaCl), TSE500 (0.1% SDS, 1% Triton X-100, 2 mM EDTA, 20 mM Tris-Cl (pH 8.1), 500 mM NaCl) and Buffer III (0.25 M LiCl, 1% NP-40, 1% sodium deoxycholate, 1 mM EDTA, 10 mM Tris-Cl (pH 8.1)) and then washed twice with TE (pH 8.0) for 10 min. Chromatin was eluted with elution buffer (1% SDS, 0.1 M $NaHCO_3$ (pH 8.0)) and incubated overnight at 65°C in 200 mM NaCl to reverse cross-linking. Aliquots (500 μl) were incubated at 50°C after addition of 10 μl 0.5 M EDTA, 20 μl 1 M Tris (pH 6.5) and 4 μl Proteinase K (20 mg ml^{-1}), extracted sequentially with phenol/chloroform/isoamyl alcohol. Nucleic acids were pelleted by centrifugation for 30 min at 4°C after addition of 1 μl of 20 mg ml^{-1} glycogen, 20 μl of 5 M NaCl and 500 μl of isopropanol. Pellets were washed with 70% ethanol, dried and resuspended in nuclease-free water.

qPCR of ChIP products

ChIP products were subject to qPCR using the DyNAmo HS SYBR Green qPCR Kit (F-410L, ThermoFisher scientific) with the CFX Connect Real-time PCR Detection System (Bio-Rad). Experimental values were normalized to the values of 1% input chromatin. Concentrations were estimated using the $2^{-\Delta\Delta CT}$ calculation method. The sequences of the primers are listed in Supplementary Table S2.

RNA sequencing

RNA from CS1AN cells stably expressing GFP, GFP-tagged CSB^{WT} and GFP-tagged $CSB^{UBDmut.}$ were isolated using RNeasy (QIAGEN). Library construction and sequencing were performed by Novogene. The samples were run on the NovaSeq 6000. The samples have >95% bases with Q30 and above. Samples were aligned to the reference human genome and junctions using STAR (v2.5) software. The percentage of alignment for all samples was over 95% with multi-mapping below 1.84%. The ratio of reads mapped to exon, intron and intergenic was in the range of 95%, 4% and 1%, respectively. Differential expression analysis between two groups (three biological replicates per group) was performed using the DESeq2 R package. The resulting *P*-values were adjusted using the Benjamini and Hochberg's approach for controlling the false discovery rate (FDR). PANTHER Classification System was used for GO analysis (http://www.geneontology.org/). Only genes that were differentially expressed with WT CSB expression but not with CSB UBD mutant expression were used for analysis. Differential expression significant analysis of two groups with three biological replicates was performed, while the significant criterion is padj (corrected *P*-value) <0.05. The following parameters were used for GO analysis. PANTHER Analysis Type: PANTHER Overrepresentation Test (Released 20181003); Annotation Version and Release Date: GO Ontology database Released 2018-09-06; Analyzed List - Sample (Homo sapiens); Reference List - Homo sapiens (all genes in database); Annotation Data Set: GO biological process complete; Test Type: The Binomial test with False Discovery Rate. The top 50 GO Biological Processes UP or DOWN-Regulated are listed in Supplementary Tables S3 and S4. GEO accession number is GEO #19587936.

←

expressed in CS1AN cells ($N = 11$–14 cells). CSB^{WT} is localized to the nucleus but is particularly enriched at the nucleolus. $CSB^{UBDmut.}$, on the other hand, is localized to nucleoplasm but appears to be enriched at the periphery of the nucleolus. Its localization to the nucleolus is impaired. (**B**) GO enrichment analysis on gene sets whose expression levels are significantly altered in CSB^{WT} but not with $CSB^{UBDmut.}$ (genes that are in the blue circle but not in the red circle were selected for further analysis.). Only Top ten GO terms are included in the figure due to lack of space. All GO terms are listed in Supplementary Tables S3 and S4. (**C**) Quantitative RT-PCR results are demonstrating the relative fold change in 47S rRNA in CS1AN cells ($CSB^{m/m}$) stably expressing either vector, CSB^{WT} or CSB^{UBDmut}. Values are from three independent biological repeats (mean ± S.E., one-way ANOVA with Tukey's post hoc test was used for statistical analysis). Western blot on the right side depicts protein expression. (**D**) Growth rates (normalized to hour 0) in CS1AN cells ($CSB^{m/m}$) stably expressing either vector, CSB^{WT} or CSB^{UBDmut}. Values are from three independent biological repeats (mean ± S.E., one-way ANOVA with Tukey's post hoc test was used for statistical analysis). (**E**) Experimental design for identifying proteins that specifically bind to CSB UBD. (**F**) Identification of Ncl by mass spectrometry. CSB-deficient CS1AN cells expressing GFP, GFP-tagged CSB^{WT} or GFP-tagged $CSB^{UBDmut.}$ were treated with Mg132 (10 μM for 2 h). Cells were lysed in IP lysis buffer. Following IP, samples were treated with USP2 (1.0 μM), separated by SDS-PAGE and visualized with silver staining. Gel slices containing higher abundance proteins were excised (arrows), and proteins were extracted/eluted from the gel. Elutes from each sliced gel were then analyzed by mass spectrometry. Western blot below the gel depicts protein expression.

Statistical analysis

One-way ANOVA with Tukey's post hoc test was used to determine significant differences across multiple samples. Two-way ANOVA with Tukey's post hoc test was used to determine significant differences across multiple samples with two groups unless indicated otherwise in figure panels. *T*-tests were used to determine the differences between the two groups. Statistical analyses were performed with GraphPad Prism version 7 (GraphPad Software, Inc.).

RESULTS

CSB binds Ncl

CSB contains a ubiquitin-binding domain (UBD), which plays an important role in DNA repair and in the cellular response to oxidative stress (6,7). CSB's localization to the nucleolus is impaired by mutations in the UBD (Figure 1A), suggesting an important role for the CSB UBD function in the nucleolus (8). To gain better insight into this, we used unbiased RNA sequencing (RNA-seq) in patient-derived CSB-deficient (CS1AN ($CSB^{m/m}$)) cells before and after correction with CSB^{WT} or $CSB^{UBDmut.}$. Since our primary focus is to investigate the function of the UBD in CSB^{WT}, we performed Gene Ontology (GO) enrichment analysis targeting the genes that are differentially expressed with CSB^{WT} but not with $CSB^{UBDmut.}$ expression. This approach helps us rule out other CSB functions that do not require UBD (Figure 1B). We find that rRNA transcription and ribosome biogenesis were among the top GO biological processes down-regulated by CSB^{WT} correction, suggesting that cells with a mutation in CSB UBD have lost the ability to regulate rRNA transcription (Figure 1B). CSB^{WT} is required for efficient synthesis of pre-rRNA (9,19). Therefore, down-regulation of genes in rRNA transcription by CSB^{WT} expression could be due to the normalization of the expression levels of the genes that are up-regulated in CSB-deficient cells. To test whether CSB UBD is necessary for CSB's regulation of rRNA transcription, we quantified the 47S rRNA levels in CS1AN cells expressing CSB^{WT} or $CSB^{UBDmut.}$. We observed that the cells expressing $CSB^{UBDmut.}$ had significantly lower 47S rRNA levels than cells expressing CSB^{WT} (Figure 1C), suggesting a role for CSB UBD in rRNA transcription. rRNA synthesis is the rate-limiting step for ribosome biogenesis, which is essential for cell growth. Therefore, we examined whether the mutation in CSB UBD affects cell proliferation. Notably, we found that stable CSB^{WT} expression in CSB-deficient cells improved cell proliferation, while $CSB^{UBDmut.}$ expression slowed proliferation even more than in CSB-deficient cells. These observations suggest that $CSB^{UBDmut.}$ expression may cause a dominant-negative effect on cell growth (Figure 1D). Given that CSB is required for maintaining a normal level of 47S rRNA and ribosome biogenesis (17,18), it suggests that CSB UBD is critical for CSB's regulation of pre-RNA synthesis and cell proliferation.

CSB UBD was initially named for its ability to bind ubiquitinated proteins (7). Here, we used immunoprecipitation (IP) assays followed by mass spectroscopy to identify proteins that specifically bind to GFP-tagged CSB^{WT}, but not to GFP-tagged $CSB^{UBDmut.}$. Polyubiquitination of proteins causes the shifting of molecular weight that makes it harder to identify precipitated proteins during silver staining on the gel. Thus, immunoprecipitated proteins were treated with USP2 (1.0 μM), a deubiquitinating enzyme, prior to gel-running (Figure 1E and Supplementary Figure S2). This experiment identified a 100 kDa protein in the CSB^{WT} immunoprecipitate that was less prominent in the $CSB^{UBDmut.}$ immunoprecipitate (Figure 1F, band #4). This protein was identified as Nucleolin (Ncl) through its peptide signature by mass spectrometry. Ncl is a ubiquitous nucleolar protein that plays an important role in rDNA transcription and ribosome biogenesis (Supplementary Table S1). The results were confirmed by performing the co-IP assay in the presence of benzonase, an enzyme that degrades DNA and RNA and prevents co-precipitation of nucleic acid-bound proteins (Figure 2A). To further validate these findings, we performed the reciprocal experiment using antibodies to CSB or Ncl to pull-down endogenous CSB or Ncl in human osteosarcoma U2OS cells (Figure 2B). We also observed that the co-localization of Ncl with CSB at the periphery of the nucleolus was impaired with the CSB UBD mutation (Figure 2C).

CSA also binds Ncl

CS patients with defects in CSA and CSB share many clinical features, suggesting that CSA and CSB play roles in similar biological pathways. However, these common pathways affected by both CSA and CSB are not well characterized. We, therefore, investigated whether CSA also interacts with Ncl. To address this, CSA-deficient CS3BE cells ($CSA^{-/-}$) or their CSA^{WT}-complemented version were transfected with plasmids expressing GFP or GFP-Ncl and the cell extracts were analyzed by GFP-IP. We found that GFP-Ncl immunoprecipitates contain a significant amount of CSA^{WT}, demonstrating that CSA binds to Ncl (Figure 3A). To ensure that this was not an artifact of CSA overexpression, we performed an endogenous CSA IP in U2OS cells and obtained similar results (Figure 3B). This is an interesting finding given that an earlier study observed that CSA localizes to the nucleoplasm and re-localizes to the nucleolus in cells treated with MG132, a proteasome inhibitor (9). As expected, treating cells with MG132 enhanced the colocalization of GFP-CSA^{WT} and endogenous Ncl in the nucleolus (Figure 3C). Further, reciprocal co-immunoprecipitation of CSA and Ncl also increased in the presence of MG132 (Figure 3D–F). These results suggest the intriguing possibility that CSA and CSB may form a functional complex with Ncl.

Interaction between $CSB^{UBDmut.}$, Ncl and CSA

Because Ncl binds to CSA and CSB, all three proteins may be in the complex. We investigated this possibility and the role of CSB UBD in this complex. GFP-tagged CSB^{WT} or GFP-tagged $CSB^{UBDmut.}$ were expressed in CS1AN cells, cell extracts were prepared and immunoprecipitated using an antibody to GFP and then analyzed by immunoblot (Figure 4A). In cells expressing $CSB^{UBDmut.}$, the interaction between CSB and endogenous Ncl appeared weaker and less protein was co-immunoprecipitated than in cells

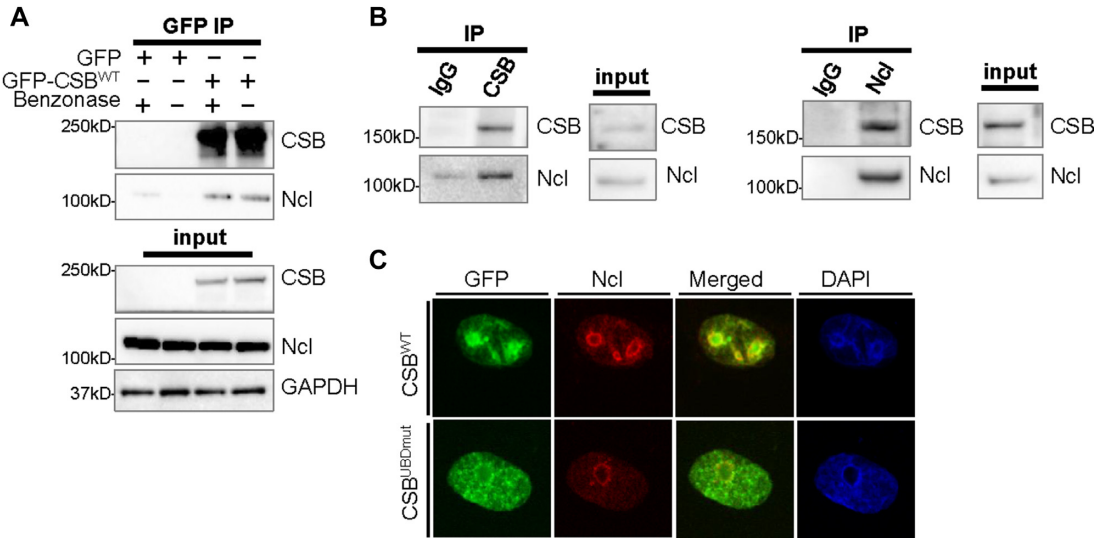

Figure 2. Ncl binds to CSB. (**A**) CSB immunoprecipitates with Ncl. CS1AN cells stably expressing GFP or GFP-CSB^{WT} were lysed and cell extracts were treated with Benzonase (1 U/ml). Samples were analyzed by western blot as described in 'Materials and Methods' section. (**B**) Endogenous interaction between Ncl and CSB in U2OS cells. U2OS cell extracts were immunoprecipitated with anti-Ncl or anti-CSB. Western blot is the representation of three independent biological repeats for CSB IP and two independent biological repeats for Ncl IP. (**C**) Co-localization of Ncl, CSB^{WT} and CSB^{UBDmut}. CS1AN cells stably expressing GFP-CSB^{WT} or GFP CSB$^{UBDmut.}$ were stained with anti-Ncl ($N = 11–14$ cells).

expressing CSB^{WT} (Figure 4A and B); in contrast, CSA appears to interact similarly with CSB^{WT} and CSB$^{UBDmut.}$ (Figure 4A). This suggests that CSB binds to CSA independently of Ncl, but that CSB UBD is required for CSB's interaction with Ncl.

As previously mentioned, CSA is a component of the E3 ligase complex, and thus recruits target proteins for ubiquitination and proteasomal degradation (25,26). Therefore, we determined the effect of CSA on the ubiquitination of Ncl. CSA-deficient CS3BE cells or their CSA^{WT}-complemented version were transfected with plasmids expressing GFP or GFP-Ncl. Cells were lysed and harvested under conditions that prevent deubiquitination (Figure 4C), and the GFP immunoprecipitates were analyzed for ubiquitination. Indeed, the results clearly indicate that CSA promotes the ubiquitination of Ncl (Figure 4C and D). It is generally thought that polyubiquitination target proteins for proteasomal degradation. However, we did not observe any stability change in Ncl with CSA expression during 8 h of proteasome inhibition (Supplementary Figure S3). We wondered whether the ubiquitination of Ncl by CSA was important for the previously identified interactions between CSB, CSA and Ncl. We, therefore, tested the potential role of CSA in maintaining or promoting the interaction between CSB and Ncl. Interestingly, we observed that CSA stimulates the interaction between CSB and Ncl (Figure 4E and F). We further determined that this was not simply due to an interaction between CSA and CSB, because CSA, compared to Ncl, pulls down very little CSB under these conditions (Supplementary Figure S4). Indeed, the interaction between CSA and CSB has been reported to be somewhat weak and perhaps transient (25,27). Thus, our results suggest that CSA enhances the interaction between CSB and Ncl. Finally, we tested whether CSA's interaction with Ncl is CSB dependent. Immunoprecipitation of endogenous Ncl with CSA in CSB deficient cells demonstrated that Ncl co-IP'ed with CSA even in the absence of functional CSB^{WT} suggesting that the interaction between CSA and Ncl is CSB independent (Figure 4G).

CSA and CSB promote binding of Ncl to rDNA and regulate pre-rRNA expression levels

We next examined the abundance of 47S rRNA in U2OS cells depleted for CSA, CSB or Ncl (Figure 5A). The depletion of CSA, CSB or Ncl caused a dramatic decrease in the abundance of 47S rRNA (Figure 5A). However, we did not observe a further reduction of 47S rRNA abundance in CSA or CSB depleted cells with additional Ncl depletion, suggesting that Ncl and CSA/CSB proteins are functioning in the same pathway in the context of 47S rRNA synthesis (Figure 5A). We also quantified 47S rRNA in CSB$^{m/m}$ cells expressing CSB^{WT} or CSB$^{UBDmut.}$ with or without depletion of Ncl (Figure 5B and Supplementary Figure S5). The results show that the depletion of Ncl severely decreases 47S rRNA in CS1AN cells stably expressing CSB^{WT}, suggesting that Ncl is required for CSB to enhance 47S rRNA transcription. Notably, the expression of CSB$^{UBDmut.}$ did not affect the abundance of 47S rRNA, and Ncl depletion in those cells did not cause any significant reduction in 47S rRNA levels (Figure 5B). These results suggest that the Ncl and CSB association is important for the regulation of pre-rRNA synthesis.

It has been reported that Ncl binds to the promoter and coding regions of rDNA and stimulates rDNA transcription (28). Therefore, we used ChIP assays to examine the distribution of Ncl on rDNA in CSB-deficient CS1AN cells and in CSA-deficient CS3BE cells with primers specific for the rDNA promoter, the coding region, as well as for a non-coding intergenic spacer (IGS) (Figure 6A). Strikingly, defi-

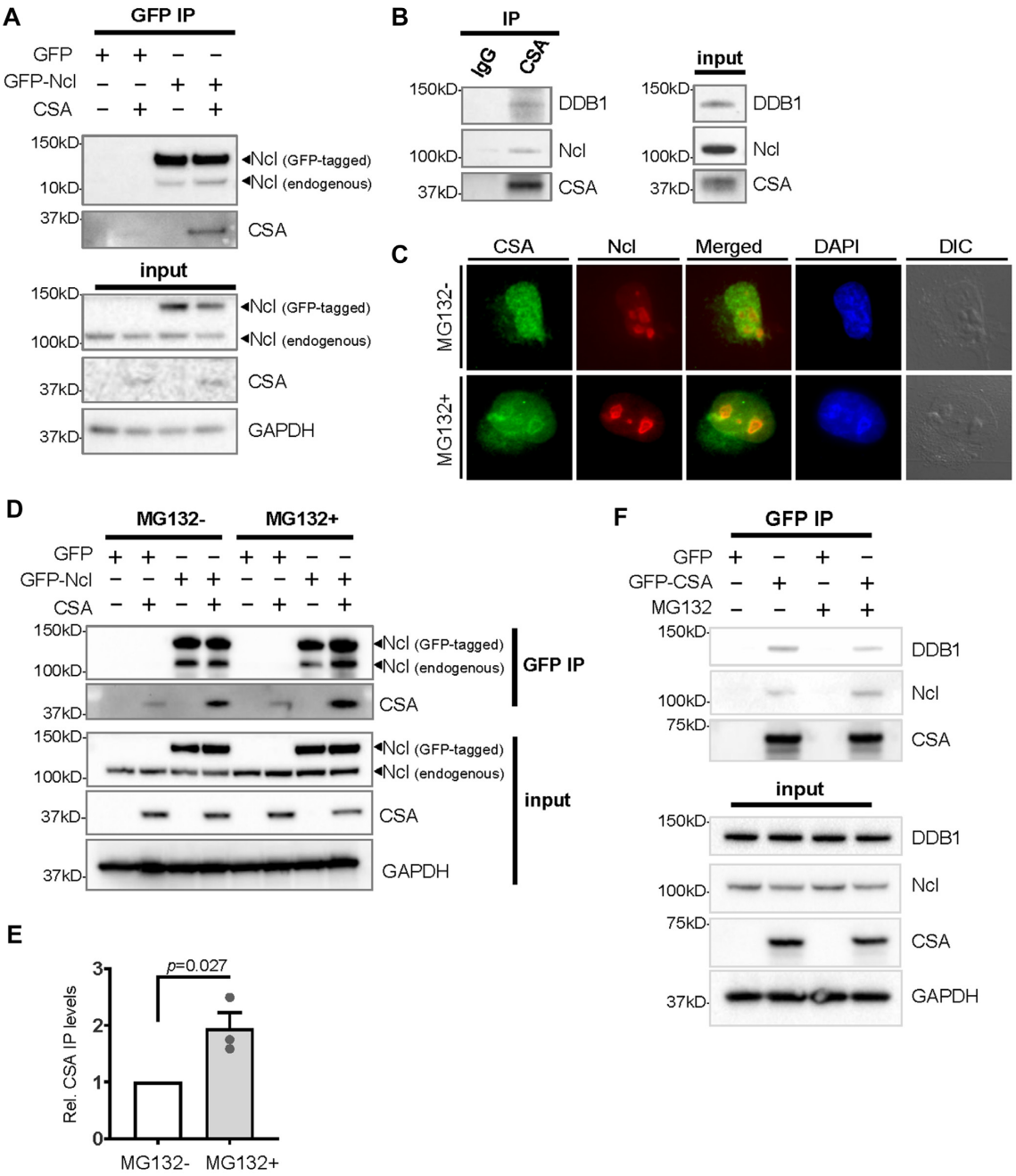

Figure 3. Ncl binds to CSA. (**A**) Interaction between CSA and Ncl. GFP-Ncl and CSA^{WT} co-immunoprecipitate (in the presence of Benzonase (1 U/ml)) from extracts of CS3BE cells, with or without complementation with CSA^{WT}, following 24H of transient transfection of plasmids expressing GFP or GFP-tagged Ncl. Western blot is the representation of three independent biological repeats. (**B**) Endogenous interaction between Ncl and CSA in U2OS cells. Whole-cell extracts were analyzed by IP using anti-CSA, as described in 'Materials and Methods' section. DDB1 is used for IP control. Western blot is the representation of three independent biological repeats. (**C**) Co-localization of Ncl and CSA in samples treated with proteasome inhibitor, MG132. Representative images of Ncl and GFP-tagged CSA in CS3BE cells treated with MG132 (24 h, 0.25 μM) ($N = 10$–12). (**D**) CSA co-immunoprecipitates with Ncl in cells treated with proteasome inhibitor, MG132. CS3BE cells, with or without complementation with CSA^{WT}, were transfected with plasmids expressing GFP or GFP-tagged Ncl. Cells were treated with MG132 (0.25 μM, 24 h), harvested and analyzed by IP, as described in 'Materials and Methods' section. (**E**) The graph shows the average signal for relative precipitated CSA/Ncl in Figure 3D (mean ± S.E., two-tailed unpaired *t*-test for comparison between groups). Quantification was done using the NIH ImageJ program. The values are the average of three independent biological repeats. (**F**) Endogenous Ncl co-immunoprecipitates with CSA in cells treated with proteasome inhibitor, MG132. CS3BE cells were transfected with plasmids expressing GFP or GFP-tagged CSA. Cells were treated with MG132 (0.25 μM, 24 h), harvested and analyzed by IP, as described in 'Materials and Methods' section. Western blot is the representation of two independent biological repeats.

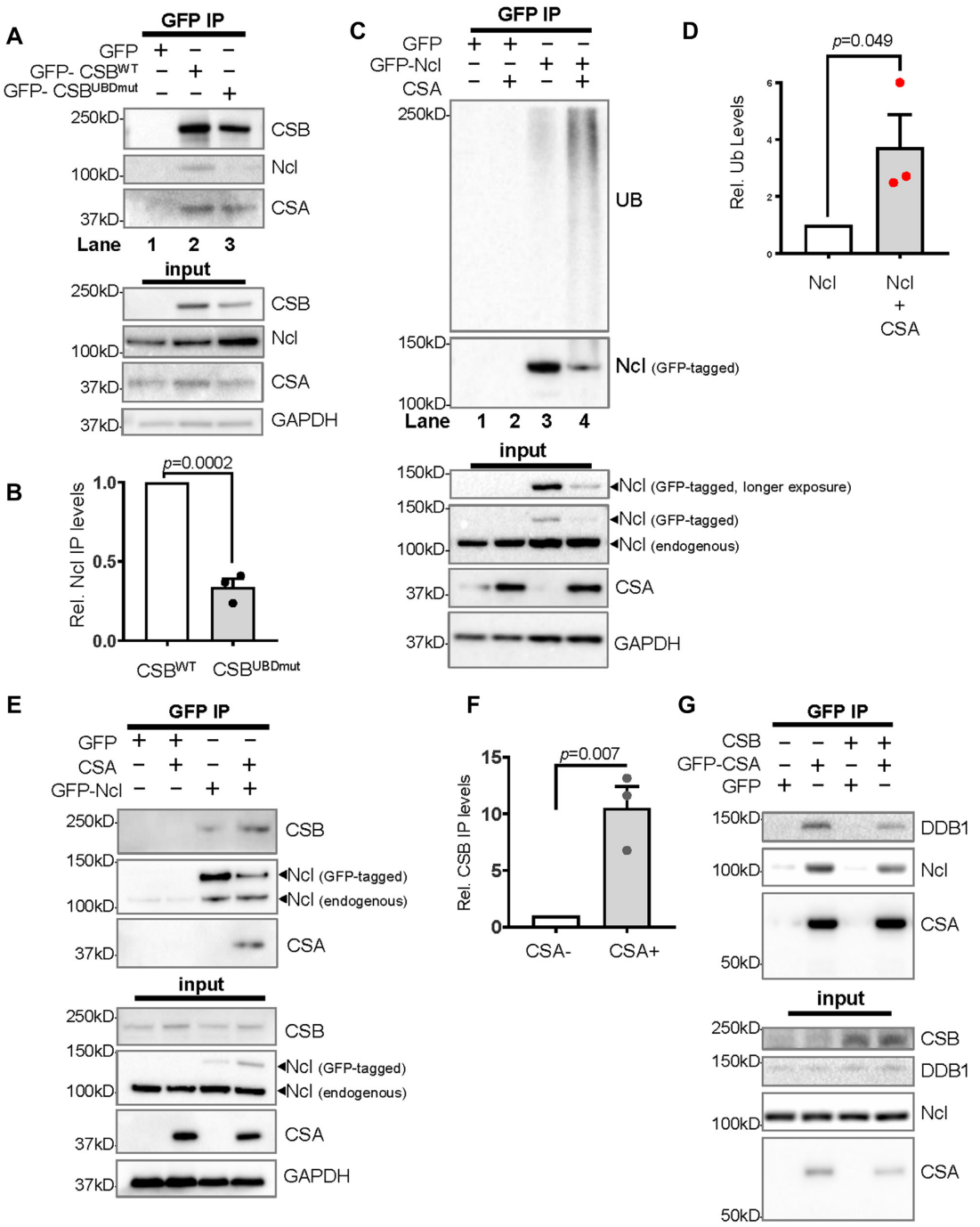

Figure 4. CSA enhances the binding of CSB to Ncl. (**A**) CS1AN cells stably expressing vector, GFP-tagged CSB^{WT} or GFP-tagged CSB$^{UBDmut.}$ were treated with Mg132 (10 μM, 2 h) prior to harvesting in IP lysis buffer. IP was performed as described in 'Materials and Methods' section. (**B**) Relative immunoprecipitated Ncl levels. The graph shows an average signal for relative precipitated Ncl/CSB in Lane 2 (CSB^{WT}) versus Lane 3 (CSB$^{UBDmut.}$) in Figure 4A (mean ± S.E., two-tailed unpaired *t*-test for comparison between groups). Densitometry quantification was done using the NIH ImageJ program. The values are the average of three independent biological repeats. (**C**) CS3BE cells or CS3BE cells complemented with CSA^{WT} were transfected with GFP-tagged Ncl, incubated for 24 h, treated with Mg132 (10 μM, 2 h) and lysed in IP lysis buffer. IP was performed using anti-GFP antibody and IP pellets were analyzed for Ub, Ncl and CSA. (**D**) Relative ubiquitination of Ncl. The graph shows the average signal for ubiquitin in Lane 3 (Ncl) versus Lane 4 (Ncl + CSA) in Figure 4C (mean ± S.E., one-tailed unpaired *t*-test for comparison between two groups). Quantification was done using the NIH ImageJ program. The values are the average of three independent biological repeats. (**E**) Immunoprecipitations as in panel (C), except IP pellets were analyzed by immunoblot using antibodies to CSB, CSA and Ncl. This experiment is repeated twice. (**F**) The graph shows the average signal for relative precipitated CSB/Ncl in Figure 4E (mean ± S.E., two-tailed unpaired *t*-test for comparison between groups). Quantification was done using the NIH ImageJ program. The values are the average of three independent biological repeats. (**G**) IP experiment is showing the interaction of CSA and Ncl in the presence or absence of CSB^{WT} in CS1AN patient-derived fibroblasts. Western blot is the representation of two independent biological repeats.

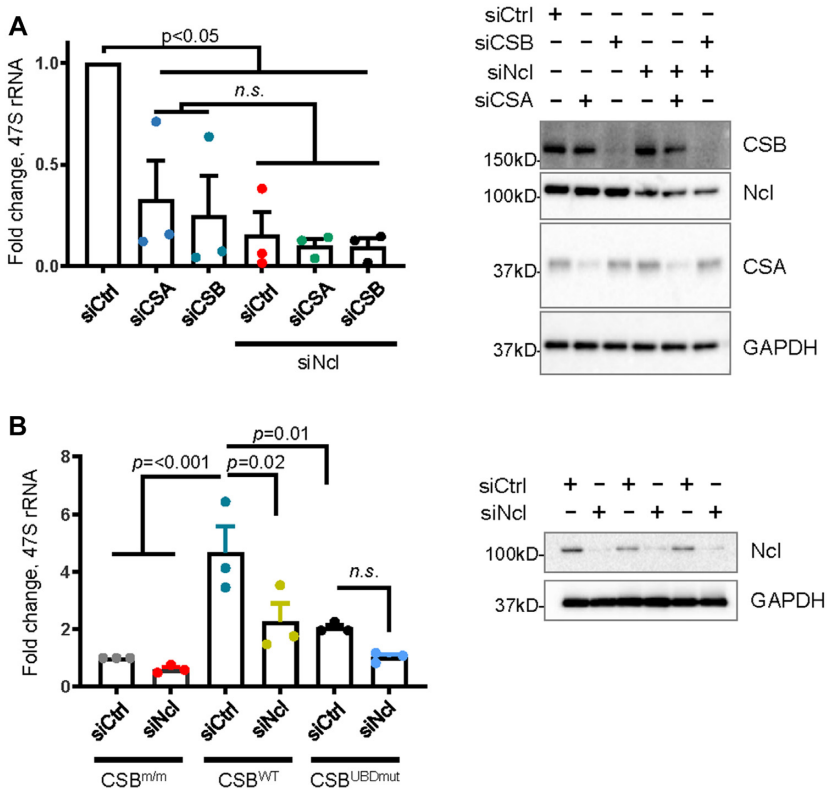

Figure 5. CSA, CSB, and Ncl promote pre-rRNA synthesis. (**A**) 47S rRNA was quantified by RT–qPCR. U2OS cells were treated with siRNA to deplete the indicated proteins. The graph shows the mean of three independent biological repeats (mean ± S.E., Two-way ANOVA with Tukey's post hoc test was used for statistical analysis). Western blot data confirm the efficiency of target protein depletion by siRNA as indicated. (**B**) As in panel (A), except CS1AN cells stably expressing vector, GFP-CSB^{WT} or GFP CSB$^{UBDmut.}$ plus or minus treatment with siRNA targeting Ncl (siNcl #1). The graph shows the mean of three independent biological repeats (mean ± S.E., Two-way ANOVA with Tukey's post hoc test was used for statistical analysis.). Western blot confirms the efficiency of the siRNA depletion of Ncl.

ciencies of either CSA or CSB led to a reduced occupancy of Ncl on the coding region of rDNA (H8 primers) (Figure 6B and C). This suggests that CSA and CSB promote Ncl binding to the coding region of rDNA to enhance transcription. The gene-internal binding of CSB and Ncl on rDNA suggests that they play a role in Pol I regulation (18,28). Thus, we next assessed Pol I binding to rDNA in Ncl depleted cells in the presence or absence of CSB^{WT}. We observed a significant increase in Pol I loading to the 3′ end of the rDNA coding region (H13) with CSB^{WT} expression (Figure 6D). Interestingly, the depletion of Ncl in CSB^{WT} expressing cells did not alter Pol I loading significantly (Figure 6D, compare CSB^{WT} and CSB^{WT} & siNcl at the H13 region). However, Ncl has been shown to induce Pol I binding to the beginning of the coding region (28), so we assessed the relative Pol I distribution on rDNA. CSB^{WT} expression led to a significant Pol I enrichment on the coding region (H13), which was reversed with Ncl depletion (Figure 6E). We observed a similar phenomenon in CS3BE cells as CSA^{WT} expression significantly increased Pol I binding to the coding region, while depletion of Ncl failed to reduce this loading (Figure 6F, compare CSA^{WT} and CSA^{WT} & siNcl at H13 region). Further, like in CSB^{WT}-deficient CS1AN cells, relative Pol I distribution on rDNA at the end of the coding region increased with CSA expression, which was also Ncl dependent (Figure 6G). The increase in Pol I binding on the H13 region may be due to enhanced elongation or Pol I stalling. To address this, we examined rDNA transcription at H13.1, which is immediately downstream of H13. We found that both CSB^{WT} or CSA^{WT} expression increased the transcript levels from the H13.1 region and that this increase was reversed after Ncl depletion (Figure 6H and I). This suggests that CSA and CSB together with Ncl induce Pol I elongation, leading to increased transcription of rDNA.

DISCUSSION

Recent reports indicate that CSA and CSB promote rDNA transcription, which is the first and rate-limiting step in ribosome biogenesis (29). However, whether there is a common mechanism involving CSA and CSB together in the regulation of rDNA transcription has not been explored. Here, we present novel evidence demonstrating the converging roles of CSA and CSB proteins in the regulation of Ncl, a key protein for rDNA transcription and pre-rRNA synthesis (Figure 7). A recent report shows that CSA relocalizes from the nucleoplasm to the nucleolus when the proteasome is inhibited with MG132 (9). We have confirmed these previous findings and we also found that CSA and Ncl interaction is present in the absence of proteasome inhibition (Figure 3D–F), suggesting that this interaction is not dependent upon MG132 treatment. This present study

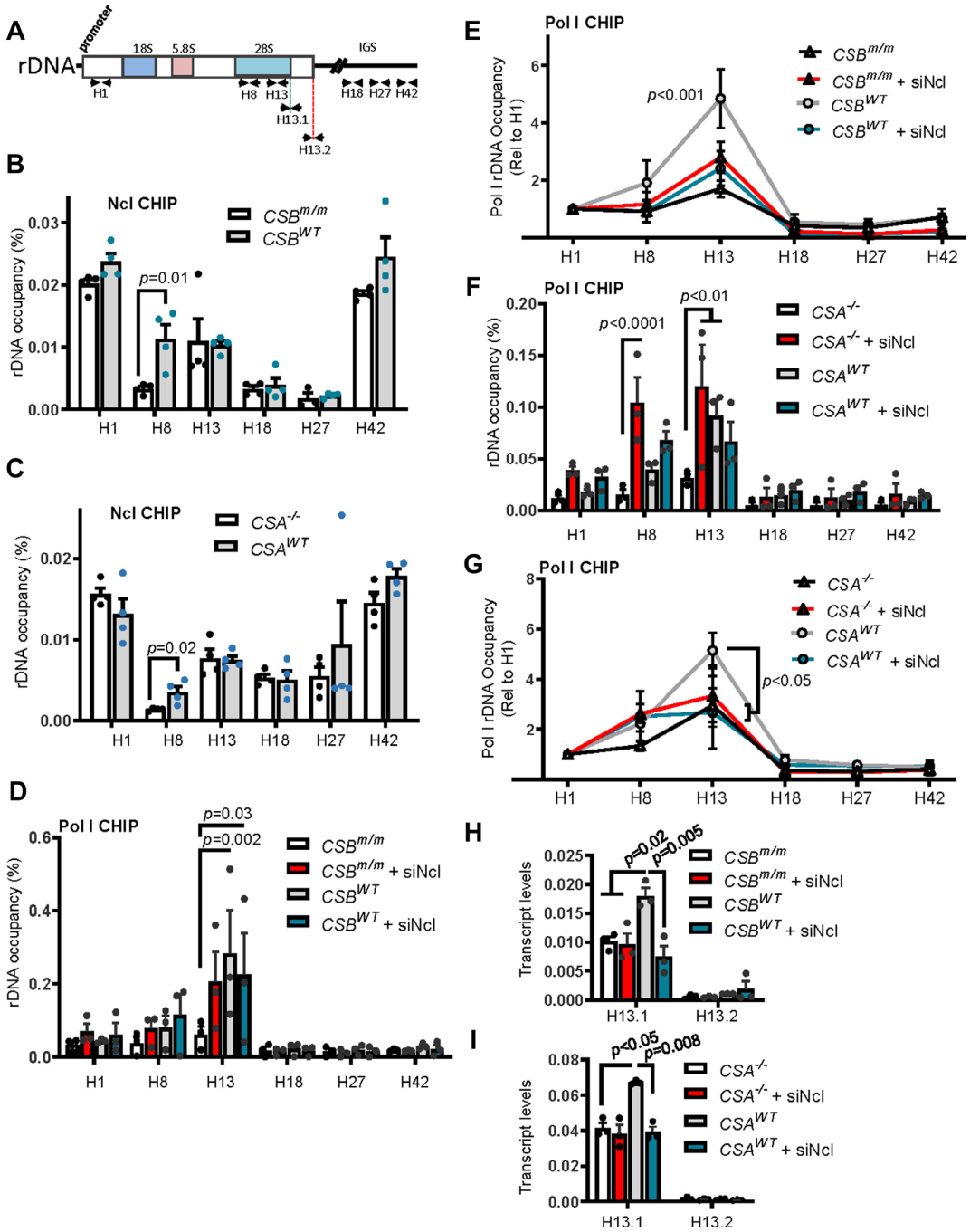

Figure 6. CSA, CSB and Ncl regulate rDNA transcription. (**A**) Schema representing a human rDNA repeat and positions of the primers used for ChIP assays. IGS stands for Spacer DNA or Intergenic Spacer. (**B** and **C**) ChIP analysis was performed using the antibody to Ncl on extracts of CS1AN cells or CS1AN cells expressing CSB^{WT} (B), or CS3BE cells or CS3BE cells expressing CSA^{WT} (C). The graph shows the mean of four independent biological repeats (mean ± S.E., two-tailed unpaired *t*-test for comparison between two groups). See 'Materials and Methods' section for details. (**D**) ChIP analysis is showing Pol I (RPA116) binding to rDNA in CSB deficient or CSB^{WT} corrected patient-derived fibroblasts following Ncl depletion. The graph shows the mean of four independent biological repeats (mean ± S.E., two-way repeated-measures ANOVA with Tukey's post hoc test was used for statistical analysis). (**E**) The graph demonstrates Pol I (RPA116) binding to rDNA that is normalized to the H1 region. The graph shows the mean of four independent biological repeats (mean ± S.E., two-way repeated-measures ANOVA with Tukey's post hoc test was used for statistical analysis). (**F**) ChIP analysis is showing Pol I (RPA116) binding to rDNA in CSA deficient or CSA^{WT} corrected patient-derived fibroblasts following Ncl depletion. The graph shows the mean of three independent biological repeats (mean ± S.E., two-way repeated-measures ANOVA with Tukey's post hoc test was used for statistical analysis). (**G**) The graph demonstrates Pol I (RPA116) binding to rDNA that is normalized to the H1 region. The graph shows the mean of three independent biological repeats (mean ± S.E., two-way repeated-measures ANOVA with Tukey's post hoc test was used for statistical analysis). (**H–I**) The graph demonstrates RT-qPCR analysis with primers spanning the gene-internal region, which is transcribed but not processed (H13.1). H13.2 primers span a region of transcribed and non-transcribed rDNA and are used as a negative control for RT-qPCR. Two-way ANOVA with Tukey's post hoc test was used for statistical analysis.

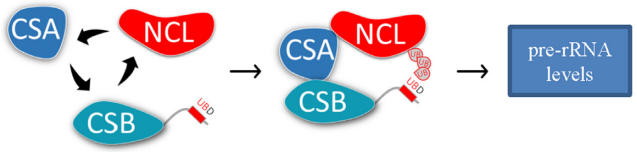

Figure 7. Graphical abstract visualizing CSA and CSB regulation of Ncl. CSA enhances Ncl ubiquitination and promotes Ncl interaction with CSB. The interplay between Ncl, CSA and CSB regulates pre-rRNA levels in the cell.

also demonstrated that CSB UBD is required for its interaction with Ncl. The polyubiquitination of proteins usually leads to degradation through the proteasome pathway. However, in the case of Ncl, its stability does not appear to be influenced by the expression of CSA (Supplementary Figure S3). Instead, CSA enhances the binding of Ncl to CSB. This leads us to speculate that the CSA ubiquitination of Ncl increases Ncl binding to the CSB UBD. Further, our results showed that transient depletion of CSA, CSB or Ncl reduces the abundance of 47S precursor rRNA levels by up to 80% (Figure 5A). However, simultaneous depletion of Ncl and CSA or CSB in U2OS cells did not cause a further reduction in 47 rRNA levels, suggesting that these proteins function in the same biogenesis pathway. In accord with this, Ncl depletion also did not cause any significant reduction in 47S rRNA levels in CSB-deficient stable cell lines (CS1AN) or in cells stably expressing $CSB^{UBDmut.}$ (Figure 5B). However, a significant reduction in the abundance of 47S pre-rRNA was observed when Ncl was depleted in CSB^{WT} corrected cells, suggesting that Ncl is required for CSB to increase 47S rRNA levels and that CSA participates via ubiquitination.

Ncl is a major nucleolar protein that plays roles in multiple steps of ribosome biogenesis (30,31). A recent study reported that Ncl is strongly enriched at the promoter and coding regions of rDNA (28). Therefore, we tested whether CSA or CSB promotes the binding of Ncl to rDNA. Consistent with previous publications, we observed enrichment of Ncl at coding regions of rDNA, while binding to non-coding regions of rDNA was negligible in CSB^{WT} corrected CS1AN cells (Figure 6A) (28). Similar results were also observed in CSA^{WT}-corrected CS3BE cells except that there was a considerable amount of enrichment of Ncl in non-coding regions of rDNA such as H18 and H27 (Figure 6B). Strikingly, deficiency of CSA or CSB strongly suppressed the binding of Ncl to the H8 coding region of rDNA, suggesting that CSA and CSB together with Ncl participate in the process of transcription elongation (Figure 6B and C). Notably, Ncl was also enriched in the H42 region, which is upstream of the transcription start site (Figure 6B and C). This region also encompasses the binding sequence for CTCF, which is a binding partner of CSB and Ncl, and it regulates the epigenetic state of rDNA repeats (32–34). Further, CTCF, CSB and Ncl are ADP-ribosylated by PARP1, which alters their binding dynamics or function (33,35). Perhaps, a complex containing CSB, Ncl, Parp1 and CTCF function together to regulate gene expression including rDNA. We observed a trend of increase in Ncl binding to H42, a binding site for CTCF, with CSA^{WT} expression although it was not significant (32) (Figure 6B and C). However, CTCF has multiple binding sites on rDNA such as H37.9 or H41.1 that remain to be explored for Ncl binding to rDNA in the context of CSA and CSB (36).

Previous reports showed that Ncl depletion had a modest impact on 45S rRNA maturation (decreased by ∼10%), suggesting that CSA and CSB modulate Ncl's role in rDNA transcription to a greater extent than its role in rRNA processing (19,28). Intriguingly, CSA, CSB and Ncl were reported to regulate Pol I loading to rDNA that can be modulated by events, including (i) an increase in promoter activity that boosts overall Pol I loading into the transcribed region of rDNA; (ii) prevention of Pol I falling off from rDNA prematurely during elongation; or (iii) defects in transcription elongation due to Pol I stalling or alterations in enzyme processivity along the ribosomal DNA. Interestingly, unlike CSA or CSB, Ncl depletion enhances Pol I loading at the promoter of rDNA, indicating that it has distinct functions on modulating the rDNA promoter, different from those of CSA or CSB (9,28,37). Further, in spite of higher Pol I binding at the promoter region, Ncl depletion leads to a dramatic decrease in the transcript levels of rDNA right after the promoter region, which was also observed with CSA or CSB depletion, suggesting elongation defects as a common phenotype seen with CSA, CSB and Ncl deficiency. We observed a similar phenomenon with Ncl depletion at the coding region of rDNA (H13) in CS3BE cells. Ncl depletion had no significant impact on transcript levels at the end of the coding region despite Pol I enrichment (Figure 6F and I), suggesting the presence of impaired elongation activity causing Pol I accumulation. Our results showed that CSB^{WT} or CSA^{WT} expression led to Ncl-dependent relative Pol I enrichment at the 3′ end of the coding region (Figure 6E and G) and that this caused increased transcript levels from the H13.1 rRNA region (Figure 6H–I), suggesting that CSB^{WT} and CSA^{WT} together with Ncl promote Pol I elongation rather than cause Pol I stalling.

The chromatin state plays an important role in transcription regulation. While euchromatin markers are linked to actively transcribed genes, heterochromatin markers are generally associated with silent regions. Interestingly, Ncl and CSB draw a distinct pattern of histone modification on rDNA. For instance, Ncl depletion leads to an increase in the heterochromatin marker H3K9me2 on the promoter and coding region of rDNA, while CSB depletion results in a decrease in H3K9me2 levels on the coding region but no effect on the promoter region (28,37). Given that pre-RNA levels are reduced with either Ncl or CSB depletion, their opposite roles in histone modifications on rDNA suggest addition levels of regulation in chromatin dynamics.

Ribosome biogenesis is one of the most energy-consuming processes in the cell. Therefore, it is important that it is tightly regulated. We recently reported increased metabolic activity and mitochondrial content despite a slower growth rate in CSB-deficient cells (38). The mTOR pathway is one of the main pathways regulating mitochondrial energy production and metabolic homeostasis (39,40). Interestingly, impaired rRNA synthesis activates the mTOR pathway (41). Further, we reported that rapamycin treatment, which inhibits mTOR, corrects mitochondrial abnormalities and rescues the bioenergetic pro-

file in CSB-deficient cells (38). Perhaps, persistent mTOR activation due to impaired rRNA might be a contributing factor to the mitochondrial phenotype observed in CS cells. Further experiments will be necessary to address this.

Dysregulation of Pol I and reduced efficiency of rRNA synthesis are implicated in the etiology of several human diseases. Importantly, less efficient rRNA synthesis is associated with neurodegeneration and premature aging in Alzheimer's disease, Amyotrophic Lateral Sclerosis, Werner and Bloom syndrome, while rDNA transcription by RNA Polymerase I is reported to be upregulated in cancer cells (42–44). It has also been reported that the expression of Ncl is downregulated or dysregulated in Parkinson's disease, Alzheimer's disease and amyotrophic lateral sclerosis, while it is upregulated in cancer cells (45). Interestingly, CS patients are not cancer-prone, despite defects in TC-NER (46). On the other hand, CSB is overexpressed in many cancer cells (47). These previous findings support that CSB and Ncl are involved in similar pathways such as rDNA transcription since modulation in their expression levels leads to similar physiological outcomes. Although mutations in CSB and CSA coding genes predominantly account for CS, there are other genetic defects that can give rise to CS-like clinical features such as mutations in *XPB*, *XPD* and *XPG* genes. Interestingly, XPB and XPD are subunits of Transcription factor IIH (TFIIH), which is recruited to the rDNA and functions in transcription elongation (48). XPG, on the other hand, is found in a CSB-containing complex that promotes efficient rRNA synthesis (19). Therefore, further experiments will be required to determine whether these other CS-related proteins also function in Ncl's regulation of rRNA synthesis.

Our working hypothesis is that CSA mediates the interaction of CSB and Ncl, which in turn, enhances Ncl binding to rDNA, induces transcription of the 3′-end coding region of rDNA and subsequent pre-rRNA synthesis. Impaired rRNA synthesis is implicated in the etiology of dwarfism and hearing loss that are the cardinal symptoms of CS (49). Therefore, the novel interactions between CSB, CSA and Ncl reported here, and their role in promoting rRNA synthesis could be a critical missing link that will increase our understanding of the pathological features of CS. Indeed, a recent genome-wide association study reported that Ncl is a strong candidate gene for noise-induced hearing loss susceptibility (50). Ultimately, these insights may accelerate progress toward an effective treatment for CS.

SUPPLEMENTARY DATA

Supplementary Data are available at NAR Online.

ACKNOWLEDGEMENTS

We would like to thank Dr. Holger Bernhard Bierhoff and Dr. Ingrid Grummt for Pol I antibodies. We also thank Dr. David M. Wilson, III for generously providing plasmids mentioned in the 'Materials and Methods' section, Dr. Kotb Aly, Dr. Kyle Hoban and Dr. Mansi Babbar for their feedback on the manuscript.

FUNDING

Intramural Research Program; National Institute on Aging, NIH and Bench-to-Bedside Program; NIH Clinical Center; Luke O'Brien Foundation. Funding for open access charge: Intramural Program, National Institutes on Aging, NIH, USA.
Conflict of interest statement. None declared.

REFERENCES

1. Karikkineth,A.C., Scheibye-Knudsen,M., Fivenson,E., Croteau,D.L. and Bohr,V.A. (2017) Cockayne syndrome: Clinical features, model systems and pathways. *Ageing Res. Rev.*, **33**, 3–17.
2. Saijo,M. (2013) The role of Cockayne syndrome group A (CSA) protein in transcription-coupled nucleotide excision repair. *Mech. Ageing Dev.*, **134**, 196–201.
3. van Gool,A.J., Citterio,E., Rademakers,S., van Os,R., Vermeulen,W., Constantinou,A., Egly,J.M., Bootsma,D. and Hoeijmakers,J.H. (1997) The Cockayne syndrome B protein, involved in transcription-coupled DNA repair, resides in an RNA polymerase II-containing complex. *EMBO J.*, **16**, 5955–5965.
4. Troelstra,C., van Gool,A., de Wit,J., Vermeulen,W., Bootsma,D. and Hoeijmakers,J.H. (1992) ERCC6, a member of a subfamily of putative helicases, is involved in Cockayne's syndrome and preferential repair of active genes. *Cell*, **71**, 939–953.
5. Fousteri,M. and Mullenders,L.H. (2008) Transcription-coupled nucleotide excision repair in mammalian cells: molecular mechanisms and biological effects. *Cell Res.*, **18**, 73–84.
6. Ranes,M., Boeing,S., Wang,Y., Wienholz,F., Menoni,H., Walker,J., Encheva,V., Chakravarty,P., Mari,P.O., Stewart,A. *et al.* (2016) A ubiquitylation site in Cockayne syndrome B required for repair of oxidative DNA damage, but not for transcription-coupled nucleotide excision repair. *Nucleic Acids Res.*, **44**, 5246–5255.
7. Anindya,R., Mari,P.O., Kristensen,U., Kool,H., Giglia-Mari,G., Mullenders,L.H., Fousteri,M., Vermeulen,W., Egly,J.M. and Svejstrup,J.Q. (2010) A ubiquitin-binding domain in Cockayne syndrome B required for transcription-coupled nucleotide excision repair. *Mol. Cell*, **38**, 637–648.
8. Iyama,T. and Wilson,D.M. 3rd. (2016) Elements that regulate the dna damage response of proteins defective in cockayne syndrome. *J. Mol. Biol.*, **428**, 62–78.
9. Koch,S., Gonzalez,Garcia, Assfalg,O., Schelling,R., Schafer,A., Scharffetter-Kochanek,P. and Iben,S. (2014) Cockayne syndrome protein A is a transcription factor of RNA polymerase I and stimulates ribosomal biogenesis and growth. *Cell Cycle*, **13**, 2029–2037.
10. Melese,T. and Xue,Z. (1995) The nucleolus: an organelle formed by the act of building a ribosome. *Curr. Opin. Cell Biol.*, **7**, 319–324.
11. Thomson,E., Ferreira-Cerca,S. and Hurt,E. (2013) Eukaryotic ribosome biogenesis at a glance. *J. Cell Sci.*, **126**, 4815–4821.
12. James,A., Wang,Y., Raje,H., Rosby,R. and DiMario,P. (2014) Nucleolar stress with and without p53. *Nucleus*, **5**, 402–426.
13. Tsekrekou,M., Stratigi,K. and Chatzinikolaou,G. (2017) The Nucleolus: In Genome Maintenance and Repair. *Int. J. Mol. Sci.*, **18**, doi:10.3390/ijms18071411.
14. Rieker,C., Engblom,D., Kreiner,G., Domanskyi,A., Schober,A., Stotz,S., Neumann,M., Yuan,X., Grummt,I., Schutz,G. *et al.* (2011) Nucleolar disruption in dopaminergic neurons leads to oxidative damage and parkinsonism through repression of mammalian target of rapamycin signaling. *J. Neurosci.*, **31**, 453–460.
15. Parlato,R. and Kreiner,G. (2013) Nucleolar activity in neurodegenerative diseases: a missing piece of the puzzle? *J. Mol. Med. (Berl)*, **91**, 541–547.
16. Alupei,M.C., Maity,P., Esser,P.R., Krikki,I., Tuorto,F., Parlato,R., Penzo,M., Schelling,A., Laugel,V., Montanaro,L. *et al.* (2018) Loss of proteostasis is a pathomechanism in cockayne syndrome. *Cell Rep.*, **23**, 1612–1619.
17. Scheibye-Knudsen,M., Tseng,A., Borch Jensen,M., Scheibye-Alsing,K., Fang,E.F., Iyama,T., Bharti,S.K., Marosi,K., Froetscher,L., Kassahun,H. *et al.* (2016) Cockayne syndrome group A and B proteins converge on transcription-linked resolution of non-B DNA. *Proc. Natl. Acad. Sci. U.S.A.*, **113**, 12502–12507.

18. Lebedev,A., Scharffetter-Kochanek,K. and Iben,S. (2008) Truncated Cockayne syndrome B protein represses elongation by RNA polymerase I. *J. Mol. Biol.*, **382**, 266–274.
19. Bradsher,J., Auriol,J., de Santis,L.P., Iben,S., Vonesch,J.L., Grummt,I. and Egly,J.M. (2002) CSB is a component of RNA pol I transcription. *Mol. Cell*, **10**, 819–829.
20. Tajrishi,M.M., Tuteja,R. and Tuteja,N. (2011) Nucleolin: The most abundant multifunctional phosphoprotein of nucleolus. *Commun. Integr Biol.*, **4**, 267–275.
21. Martin,N.P., Mohney,R.P., Dunn,S., Das,M., Scappini,E. and O'Bryan,J.P. (2006) Intersectin regulates epidermal growth factor receptor endocytosis, ubiquitylation, and signaling. *Mol. Pharmacol.*, **70**, 1643–1653.
22. Okur,M.N., Ooi,J., Fong,C.W., Martinez,N., Garcia-Dominguez,C., Rojas,J.M., Guy,G. and O'Bryan,J.P. (2012) Intersectin 1 enhances Cbl ubiquitylation of epidermal growth factor receptor through regulation of Sprouty2-Cbl interaction. *Mol. Cell Biol.*, **32**, 817–825.
23. Lee,J.H., Kang,B.H., Jang,H., Kim,T.W., Choi,J., Kwak,S., Han,J., Cho,E.J. and Youn,H.D. (2015) AKT phosphorylates H3-threonine 45 to facilitate termination of gene transcription in response to DNA damage. *Nucleic Acids Res.*, **43**, 4505–4516.
24. Seither,P. and Grummt,I. (1996) Molecular cloning of RPA2, the gene encoding the second largest subunit of mouse RNA polymerase I. *Genomics*, **37**, 135–139.
25. Groisman,R., Kuraoka,I., Chevallier,O., Gaye,N., Magnaldo,T., Tanaka,K., Kisselev,A.F., Harel-Bellan,A. and Nakatani,Y. (2006) CSA-dependent degradation of CSB by the ubiquitin-proteasome pathway establishes a link between complementation factors of the Cockayne syndrome. *Genes Dev.*, **20**, 1429–1434.
26. Latini,P., Frontini,M., Caputo,M., Gregan,J., Cipak,L., Filippi,S., Kumar,V., Velez-Cruz,R., Stefanini,M. and Proietti-De-Santis,L. (2011) CSA and CSB proteins interact with p53 and regulate its Mdm2-dependent ubiquitination. *Cell Cycle*, **10**, 3719–3730.
27. Licht,C.L., Stevnsner,T. and Bohr,V.A. (2003) Cockayne syndrome group B cellular and biochemical functions. *Am. J. Hum. Genet.*, **73**, 1217–1239.
28. Cong,R., Das,S., Ugrinova,I., Kumar,S., Mongelard,F., Wong,J. and Bouvet,P. (2012) Interaction of nucleolin with ribosomal RNA genes and its role in RNA polymerase I transcription. *Nucleic Acids Res.*, **40**, 9441–9454.
29. Gourse,R.L., Gaal,T., Bartlett,M.S., Appleman,J.A. and Ross,W. (1996) rRNA transcription and growth rate-dependent regulation of ribosome synthesis in Escherichia coli. *Annu. Rev. Microbiol.*, **50**, 645–677.
30. Fremerey,J., Morozov,P., Meyer,C., Garzia,A., Teplova,M., Tuschl,T. and Borkhardt,A. (2016) Nucleolin controls ribosome biogenesis through its RNA-Binding properties. *Blood*, **128**, 5056.
31. Ginisty,H., Amalric,F. and Bouvet,P. (1998) Nucleolin functions in the first step of ribosomal RNA processing. *EMBO J.*, **17**, 1476–1486.
32. Todd,M.A., Huh,M.S. and Picketts,D.J. (2016) The sub-nucleolar localization of PHF6 defines its role in rDNA transcription and early processing events. *Eur. J. Hum. Genet.*, **24**, 1453–1459.
33. Witcher,M. and Emerson,B.M. (2009) Epigenetic silencing of the p16(INK4a) tumor suppressor is associated with loss of CTCF binding and a chromatin boundary. *Mol. Cell*, **34**, 271–284.
34. Lake,R.J., Boetefuer,E.L., Won,K.J. and Fan,H.Y. (2016) The CSB chromatin remodeler and CTCF architectural protein cooperate in response to oxidative stress. *Nucleic Acids Res.*, **44**, 2125–2135.
35. Thorslund,T., von Kobbe,C., Harrigan,J.A., Indig,F.E., Christiansen,M., Stevnsner,T. and Bohr,V.A. (2005) Cooperation of the Cockayne syndrome group B protein and poly(ADP-ribose) polymerase 1 in the response to oxidative stress. *Mol. Cell Biol.*, **25**, 7625–7636.
36. van de Nobelen,S., Rosa-Garrido,M., Leers,J., Heath,H., Soochit,W., Joosen,L., Jonkers,I., Demmers,J., van der Reijden,M., Torrano,V. *et al.* (2010) CTCF regulates the local epigenetic state of ribosomal DNA repeats. *Epigenetics Chromatin*, **3**, 19.
37. Yuan,X., Feng,W., Imhof,A., Grummt,I. and Zhou,Y. (2007) Activation of RNA polymerase I transcription by cockayne syndrome group B protein and histone methyltransferase G9a. *Mol. Cell*, **27**, 585–595.
38. Scheibye-Knudsen,M., Ramamoorthy,M., Sykora,P., Maynard,S., Lin,P.C., Minor,R.K., Wilson,D.M. 3rd, Cooper,M., Spencer,R., de Cabo,R. *et al.* (2012) Cockayne syndrome group B protein prevents the accumulation of damaged mitochondria by promoting mitochondrial autophagy. *J. Exp. Med.*, **209**, 855–869.
39. Saxton,R.A. and Sabatini,D.M. (2017) mTOR signaling in growth, metabolism, and disease. *Cell*, **168**, 960–976.
40. Morita,M., Gravel,S.P., Hulea,L., Larsson,O., Pollak,M., St-Pierre,J. and Topisirovic,I. (2015) mTOR coordinates protein synthesis, mitochondrial activity and proliferation. *Cell Cycle*, **14**, 473–480.
41. Liu,R., Iadevaia,V., Averous,J., Taylor,P.M., Zhang,Z. and Proud,C.G. (2014) Impairing the production of ribosomal RNA activates mammalian target of rapamycin complex 1 signalling and downstream translation factors. *Nucleic Acids Res.*, **42**, 5083–5096.
42. Barna,M., Pusic,A., Zollo,O., Costa,M., Kondrashov,N., Rego,E., Rao,P.H. and Ruggero,D. (2008) Suppression of Myc oncogenic activity by ribosomal protein haploinsufficiency. *Nature*, **456**, 971–975.
43. Ruggero,D. and Pandolfi,P.P. (2003) Does the ribosome translate cancer? *Nat. Rev. Cancer*, **3**, 179–192.
44. White,R.J. (2005) RNA polymerases I and III, growth control and cancer. *Nat. Rev. Mol. Cell Biol.*, **6**, 69–78.
45. Drygin,D., Siddiqui-Jain,A., O'Brien,S., Schwaebe,M., Lin,A., Bliesath,J., Ho,C.B., Proffitt,C., Trent,K., Whitten,J.P. *et al.* (2009) Anticancer activity of CX-3543: A direct inhibitor of rRNA biogenesis. *Cancer Res.*, **69**, 7653–7661.
46. Reid-Bayliss,K.S., Arron,S.T., Loeb,L.A., Bezrookove,V. and Cleaver,J.E. (2016) Why Cockayne syndrome patients do not get cancer despite their DNA repair deficiency. *Proc. Natl. Acad. Sci. U.S.A.*, **113**, 10151–10156.
47. Caputo,M., Frontini,M., Velez-Cruz,R., Nicolai,S., Prantera,G. and Proietti-De-Santis,L. (2013) The CSB repair factor is overexpressed in cancer cells, increases apoptotic resistance, and promotes tumor growth. *DNA Repair*, **12**, 293–299.
48. Nonnekens,J., Perez-Fernandez,J., Theil,A.F., Gadal,O., Bonnart,C. and Giglia-Mari,G. (2013) Mutations in TFIIH causing trichothiodystrophy are responsible for defects in ribosomal RNA production and processing. *Hum. Mol. Genet.*, **22**, 2881–2893.
49. Hannan,K.M., Sanij,E., Rothblum,L.I., Hannan,R.D. and Pearson,R.B. (2013) Dysregulation of RNA polymerase I transcription during disease. *Biochim. Biophys Acta*, **1829**, 342–360.
50. Grondin,Y., Bortoni,M.E., Sepulveda,R., Ghelfi,E., Bartos,A., Cotanche,D., Clifford,R.E. and Rogers,R.A. (2015) Genetic polymorphisms associated with hearing threshold shift in subjects during first encounter with occupational impulse noise. *PLoS One*, **10**, e0130827.